Prediction of the elastic modulus of LLDPE/CNT nanocomposites by analytical modeling and finite element analysis

Charitos, Ilias; Drougkas, Anastasios; Kontou, Evagelia

DOI
10.1016/j.mtcomm.2020.101070

Publication date
2020

Document Version
Accepted author manuscript

Published in
Materials Today Communications

Citation (APA)
Charitos, I., Drougkas, A., & Kontou, E. (2020). Prediction of the elastic modulus of LLDPE/CNT nanocomposites by analytical modeling and finite element analysis. *Materials Today Communications*, *24*, Article 101070. https://doi.org/10.1016/j.mtcomm.2020.101070

Prediction of the elastic modulus of LLDPE/CNT nanocomposites by analytical modeling and finite element analysis.

Ilias Charitos[a] , Anastasios Drougkas[b], Evagelia Kontou[a*]

[a] *Mechanics Department, School of Applied Mathematical and Physical Sciences, National Technical University of Athens, Iroon Polytechniou 9, Zografou 15780, Athens, Greece*

[b] *Faculty of Civil Engineering and Geosciences, TU Delft, Stevinweg 1, 2628 CN, Delft, Netherlands*

[*]Corresponding author.

Tel: 00302107721219, E-mail address: ekontou@central.ntua.gr

Abstract

In the present work, the effective elastic modulus of carbon nanotube (CNT) polymer nanocomposites has been evaluated through micromechanics modeling and finite element analysis (FEA). In the micromechanics model, the inherent trend of CNTs to aggregate is taken into account, considering a two-phase material system, that of the matrix with the finely dispersed CNTs and the inclusions, involving agglomerated CNTs and matrix material. A new model is proposed for the elastic stiffness evaluation of the two phases and the elastic stiffness of the nanocomposite, introducing two aggregation parameters. It was proved that this analysis was rational and operative. The same aggregation concept has been investigated using FEA, and a comparative study between the two procedures was performed. Furthermore, an additional treatment with

FEA was performed, based on a three-phase model, including the matrix, the CNTs and the interphase. A parametric analysis has been executed and a comparison with experimental data of linear low density polyethylene (LLDPE)/CNT nanocomposites has been performed.

Key words: Linear low-density polyethylene; Carbon nanotube reinforced nanocomposites; Micromechanics; Finite element analysis.

1. Introduction

The remarkable mechanical properties of carbon nanotubes (CNTs), such as hardness, high strength and flexibility, low density and excellent electrical and thermal properties, have rendered them a distinguished reinforcement agent. It has been observed that the addition of 1 wt.% CNT to a matrix resulted in 36–42 % increases in the composite hardness [1,2].

Over the past few decades, CNTs, as reinforcing agents for a variety of polymeric structures, have attracted great attention because of their structure and properties. This is due to the unusual physical and mechanical properties, as a direct result of the almost perfect microstructure, namely the hexagonal sheet of carbon atoms rolled in a cylindrical shape [3-7]. As a result, CNTs have been employed in a wide range of applications such as chemical and genetic probes, mechanical memory, sensors and structural materials [3]. A lot of research has been focused on the mechanical enhancement of polymers reinforced with CNTs [3-9]. Polymer/CNT nanocomposites appear to have numerous potential advantages such as increased energy absorbance,

high toughness, easier manufacturing processing and high strength and modulus over weight ratio.

Modeling of the elastic properties of CNT/polymer nanocomposites has been the subject of numerous works [3, 6, 10-14]. Odegard et al. [10] used the Mori–Tanaka method to predict the elastic properties of CNT/polyimide composites at various lengths, orientations, and volume fractions. Seidal and Lagoudas [12] predicted the elastic properties of CNT/epoxy composites using a variety of analytical micromechanical approaches.

Anumandla and Gibson [13] presented a comprehensive micromechanical model that incorporates the effect of nanotubes' curvature, length, and their 1D/3D random orientations, to calculate the elastic modulus of CNT nanocomposites.

Mechanical properties of high-density polyethylene composites reinforced with CNTs were also presented by Kanagaraj et al. [14].

Referring to more recent works, in [15], a new form of the rule of mixtures, containing an exponential shape function, length efficiency parameter, orientation efficiency factor and a waviness parameter, was proposed to predict the mechanical properties of CNT-reinforced epoxy composites, for both low and high wt.% ranges.

In [16] the mechanical enhancement of a polymer/CNT nanocomposite was analyzed with regard to the Young's modulus and the yield strength of the interfacial region, on the basis of a three – phase micromechanical model.

In a recent work [17], the tensile modulus of polymer/CNT nanocomposites was evaluated by the Kolarik model, on the assumption of CNTs continuous networks into the polymer bulk, where the interphase surrounding the CNTs is also accounted for.

In the same trend, two models for the tensile modulus considering the dispersion and CNTs networking as well as the interphase around CNTs [18] are combined to predict the tensile modulus, as well as the effect of the model parameters.

Finite Element Analysis (FEA) has been proved to be a useful tool for studying and analyzing the mechanical performance of polymer/CNT nanocomposites [19].

FEA is particularly useful in the verification of the accuracy of micromechanics model for composite materials.

In [20] using a representative volume element (RVE), the effects of several geometrical and material parameters on the low-velocity impact behavior of nanocomposites have been studied. In addition, different impact velocities and the impact energy absorption characteristics of nanocomposites have been investigated.

In another work [21], a coupled field finite element analysis is carried out for CNT reinforced epoxy based composite subjected to thermo-mechanical loading. The effect of CNT length on the thermo-mechanical behavior was analyzed using a hexagonal RVE.

Despite these advantages of CNTs and the research that has been performed so far, there is still a need of further research to improve our understanding by developing models predicting the mechanical enhancement of polymer/CNT nanocomposites. Regarding linear low-density polyethylene (LLDPE), which is the matrix material employed in this work, there are limited studies on blending LLDPE with CNTs [6,7, 22-26].

The scope of the present work, is the prediction of the elastic stiffness of polymer /CNT nanocomposites focusing on the two main features of CNTs: Their inherent tendency to

agglomerate and the role of the interphase region around CNTs, given the large surface area between the matrix and the nanofillers. In the present work, a new version of a micromechanics model is presented for the elastic stiffness evaluation, introducing two agglomeration parameters. The nanocomposite is considered to contain a fictitious matrix, involving matrix material and dispersed CNTs, and inclusions which involve CNTs agglomerates and matrix material. The elastic stiffness of the fictitious matrix has been evaluated by Odegard's model , using the concept of the effective fiber, treated as a transversely isotropic material. A finite element analysis was also executed on the basis of these main assumptions. The accuracy of the micromechanics model has been evaluated against the FEA results.The concept of the interphase was further elaborated by FEA, through a parametric analysis within the context of a three phase model. The effect of the interphase modulus and thickness on the nanocomposites' elastic properties has been extensively analyzed. The model simulation was performed on the basis of the tensile modulus experimental results executed in our previous works [6, 7]. Specifically, two types of LLDPE reinforced with CNTs at different CNT content, were investigated, namely zLLDPE and mLLDPE produced by Ziegler-Natta and metallocene catalysts, analytically presented in [6,7].

2. Analytical Micromechanics model: Inclusion model

In this section, the Young's modulus of the LLDPE/CNT nanocomposites is analyzed, considering the inherent tendency of the nanofillers to produce agglomerates, when they are dispersed into the polymeric bulk. The elastic properties of the LLDPE/CNT

nanocmposites examined were experimentally studied in [6,7] and are presented in Table 1.

Table 1

Mechanical properties of the LLDPE/CNT nanocomposites studied, taken from ref. [6,7]

Material	CNT volume (%)	Young's Modulus (MPa)	Modulus Increment (%)	Yield stress (MPa)	Failure stress (MPa)	Yield strain (%)	Failure strain (%)
zLLDPE	-	335	-	5.6	22.7	12	1125
zLLDPE/2%CNT	0.013	430	28.3	6.8	16.7	8.4	874
zLLDPE/4%CNT	0.0262	472	40.9	7.0	18.1	10.3	871
zLLDPE/6%CNT	0.0393	477	42.4	7.5	23.2	10.0	915
zLLDPE/8%CNT	0.0525	500	49.2	8.0	18.2	12.0	682
zLLDPE/10%CNT	0.0655	600	79.1	9.7	11.9	7.7	445
zLLDPE/15%CNT	0.098	548	63.6	10.5	10.7	11.5	275
zLLDPE/20%CNT	0.131	730	118.0	11.2	10.9	8.9	125
mLLDPE	-	205	-	3.86/5.3	22.7	16.0	1036
mLLDPE/2%CNT	0.0176	261	27.3	3.77 /5.5	16.7	14.7	1187
mLLDPE/4%CNT	0.0266	302	47.3	3.23/5.8	18.1	10.1	788
mLLDPE/6%CNT	0.0360	350	70.7	5.13/7.5	23.2	20.1	708
mLLDPE/8%CNT	0.0455	363	77.1	5.41/7.8	18.2	16.3	638
mLLDPE/10%CNT	0.0879	410	100	6.0 /8.5	11.9	20.5	468

In this Table, the different mechanical performance, mainly due to the different LLDPE matrix, is revealed. In addition, mLLDPE/nanocomposites exhibit two yield stresses, as shown in Table 1 and analyzed in [7].

Several theoretical works on the prediction of the mechanical enhancement of polymer nanocomposites have been developed so far, [6, 10, 11, 14, 27, 28-30]. Following [30],

it is assumed that the nanocomposite is mainly a two – phase system. The first phase is the polymeric matrix which contains a number of dispersed CNTs and is called fictitious matrix. The second phase involves spherical regions, which contain agglomerated (concentrated) CNTs embedded in the matrix material. These phases are called inclusions. The two phases are illustrated in Figure 1. In the present work, a new analysis approach will be hereafter adopted, regarding the calculation of the elastic modulus of the involved phases.

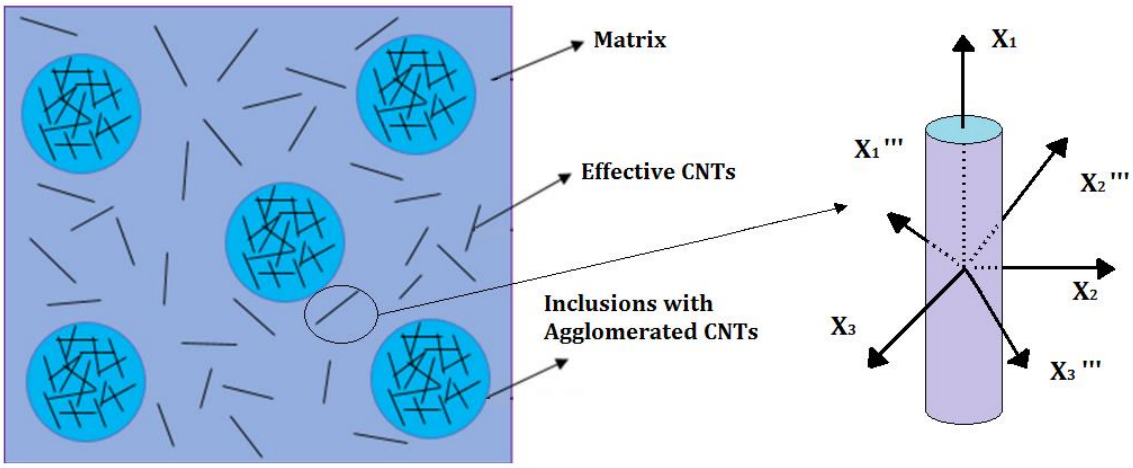

Figure 1: a) Schematic presentation of the inclusion model with agglomerated CNTs dispersed into the matrix b) Orientation of the effective CNT referring to the local $x_1x_2x_3$ and to the global $x_1'''x_2'''x_3'''$ coordinates.

2.1 Calculation of the elastic stiffness E_m^f *of the fictitious matrix*

This procedure is similar to the one, followed in our previous work [6], where the distinctive mechanical enhancement, obtained by the dispersed nanofillers, is combined with a micromechanics model, initially developed for conventional composites. Therefore, the elastic stiffness tensor **C** (of the fictitious matrix) as expressed by Mori-Tanaka [27] and later by Benveniste [11] is given by:

$$\mathbf{C} = \mathbf{C}_m + v_f \left\langle \left(\mathbf{C}_f - \mathbf{C}_m\right) A^f \right\rangle \left(v_m \mathbf{I} + v_f \left\langle \mathbf{A}^f \right\rangle\right)^{-1} \quad (1)$$

where $\mathbf{C}_m$ is the matrix stiffness tensor, $\mathbf{C}_f$ the CNT's stiffness tensor, **I** is the identity matrix tensor, v_f is the volume fraction of the fictitious matrix and $\mathbf{A}_f$ is the dilute mechanical strain concentration tensor for the CNTs:

$$\mathbf{A}_f = \left[\mathbf{I} + \mathbf{S}\left(\mathbf{C}_m\right)^{-1}\left(\mathbf{C}_f - \mathbf{C}_m\right)\right]^{-1} \quad (2)$$

where **S** is the Eshelby tensor, expressed for spheroidal inclusions [31, 32] is given by:

$$\mathbf{S} = \begin{bmatrix} s_{11} & s_{12} & s_{13} & 0 & 0 & 0 \\ s_{21} & s_{22} & s_{23} & 0 & 0 & 0 \\ s_{31} & s_{32} & s_{33} & 0 & 0 & 0 \\ 0 & 0 & 0 & s_{44} & 0 & 0 \\ 0 & 0 & 0 & 0 & s_{55} & 0 \\ 0 & 0 & 0 & 0 & 0 & s_{55} \end{bmatrix} \quad (3)$$

where

s11=(1/(2 (1-v))) (1-2 v+(3 t^2-1)/(t^2-1)-(1-2 v+3 t^2/(t^2-1)) g)

s22=s33=(3/((1-v) 8)) t^2/(t^2-1)+(1/(4 (1-v))) (1-2 v-9/(4 (t^2-1))) g

s12=s21=(1/(4 (1-v))) (t^2/(2 (t^2-1))-(1-2 v)-(3/(4 (t^2-1))) g)

s13=s23=-1/(2 (1-v)) t^2/(t^2-1)+1/(4 (1-v)) (3 t^2/(t^2-1)-(1-2 v)) g

s31=s32=-1/(2 (1-v)) (1-2 v+1/(t^2-1))+1/(2 (1-v)) (1-2 v+3/(2 (t^2-1))) g

s44=(1/(4 (1-v))) (t^2/(2 (t^2-1))+(1-2 v-3/(4 (t^2-1))) g)

s55=(1/(4 (1-v))) (1-2 v-(t^2+1)/(t^2-1)-0.5 (1-2 v-(3 t^2+3)/(t^2-1)) g)

(4)

with $g = t\,(t(t\text{^}2-1)\text{^}.5 - \text{ArcCosh}[t])/(t\text{^}2-1)\text{^}1.5$, v being the Poisson's ratio of the CNTs and t their aspect ratio. The angle brackets in eq (1) represent the average value over all possible orientation of the CNTs, as follows:

$$\bar{\mathbf{A}}^{f}_{ijkl} = c_{ip}c_{jq}c_{kr}c_{ls}\ \mathbf{A}^{f}_{pqrs} \tag{5}$$

and c_{ij} are the direction cosines for the transformation:

$$\begin{aligned}
c_{11} &= \cos\varphi\cos\psi - \sin\varphi\cos\gamma\sin\psi \\
c_{12} &= \sin\varphi\cos\psi + \cos\varphi\cos\gamma\sin\psi \\
c_{13} &= \sin\psi\sin\gamma \\
c_{21} &= -\cos\varphi\sin\psi - \sin\varphi\cos\gamma\cos\psi \\
c_{22} &= -\sin\varphi\sin\psi + \cos\varphi\cos\gamma\cos\psi \\
c_{23} &= \sin\gamma\cos\psi \\
c_{31} &= \sin\varphi\sin\gamma \\
c_{32} &= -\cos\varphi\sin\gamma \\
c_{33} &= \cos\gamma
\end{aligned} \tag{6}$$

with γ, φ, ψ being the angles for the transformation from the local effective fiber coordinates (x_1,x_2,x_3) to the global coordinates x_1''',x_2''',x_3''' (see Figure 1).

Then, the orientation average of tensor $\mathbf{A}^f$ is given by:

$$\left\langle \mathbf{A}^{f} \right\rangle = \frac{\int_{-\pi}^{\pi}\int_{0}^{\pi}\int_{0}^{\pi/2} \bar{\mathbf{A}}^{f}(\varphi,\gamma,\psi)\ \lambda(\varphi,\psi)\sin(\gamma)\,d\varphi d\gamma d\psi}{\int_{-\pi}^{\pi}\int_{0}^{\pi}\int_{0}^{\pi/2} \lambda(\varphi,\psi)\sin(\gamma)\,d\varphi d\gamma d\psi} \tag{7}$$

where $\lambda(\varphi,\psi)$ is the orientation distribution function:

$$\lambda(\varphi,\psi) = \exp\left[-s_1\varphi^2\right]\exp\left[-s_2\psi^2\right] \tag{8}$$

Parameters s_1, s_2 determine the orientation of the CNTs. The fictitious matrix is treated as an isotropic material, due to the random dispersion of the CNTs. Therefore, factors s_1, s_2 are equal to zero and consequently $\lambda(\varphi,\psi)=1$. Odegard et al. [10], introduced a coupling between the established micromechanics model and an equivalent continuum modeling method. More specifically, the nanotube, the local polymer chains around the nanotube and the CNT/polymer interface can be modeled as an effective continuum fiber. In this way, both effects, that of the agglomerate tendency of the CNTs and the specific contribution of the interphase are accounted for in the present approach. Hereafter, the elastic stiffness tensor **C**, and consequently the longitudinal modulus E_m^f of the fictitious matrix, has been evaluated. Carbon nanotubes (effective fibers) were treated as a transversely isotropic material, described by five elastic constants, namely the longitudinal elastic modulus E_1, the transverse modulus $E_2=E_3$, one shear modulus G_{12}, and the Poisson's ratios $v_{12}=v_{13}$ and v_{23}. To obtain a good approximation of the experimental data, the elastic properties of the CNTs employed are: E_1=910 GPa, $E_2=E_3$=304 GPa, $G_{12}=G_{13}$=194 GPa, $v_{12}=v_{13}$= 0.2 and v_{23}=0.3.

2.2 Calculation of the elastic stiffness E_{inc} *of the inclusion*

The elastic stiffness of the inclusions will be calculated by the empirical model by Tsai-Pagano [33, 34], with the main assumptions of a good matrix-nanofiller adhesion, good dispersion quality and random orientation of CNTs. Therefore the inclusions modulus E_{inc} is given by :

$$E_{inc}=\frac{3}{8}E_{inc}^{L}+\frac{5}{8}E_{inc}^{T} \qquad (9)$$

where E_{inc}^{L} and E_{inc}^{T} are the corresponding moduli in the longitudinal and transverse direction, which are given as follows:

$$E_{inc}^{L} = E_f \lambda V_f + E_m (\xi - \lambda V_f) \tag{10}$$

$$E_{inc}^{T} = \frac{E_m E_f}{E_m \lambda V_f + E_f (\xi - \lambda V_f)} \tag{11}$$

where ξ is the volume fraction of the inclusions into the nanocomposite and λ is the ratio of the volume fraction of CNTs into the inclusion over the total volume fraction V_f of the CNTs. It therefore follows that the E_{inc}^{L} expresses the mixture law for the iso-strain condition, and the E_{inc}^{T} represents the iso-stress condition.

Regarding agglomeration parameters ξ, λ, it can be easily shown that for the volume fraction of the fictitious matrix v_f the expression $v_f = 1-\xi$ is valid.

By definition, the values of ξ, λ are positive and lower than unity. When $\xi=1$, CNTs are uniformly distributed in the original matrix, and when $\lambda=1$ all the CNTs are embedded in the inclusions. When $\xi=\lambda$ all the CNTs are uniformly distributed in the original matrix and the inclusions [30].

2.3 Calculation of the elastic stiffness E_c of the nanocomposite

The elastic stiffness of the nanocomposite E_c is finally given by the semi-empirical model of Cox-Krenchel [35], or the modified rule of mixtures:

$$E_c = h_o h_c E_{inc} \xi + E_m^f (1-\xi) + C \quad (12)$$

where E_m^f is the elastic modulus of the fictitious matrix, h_o is a parameter denoting the CNTs orientation, which in the present case was equal to 0.2, indicating random orientation of the inclusions into the fictitious matrix. Parameter h_L is given by:

$$h_L = 1 - \frac{\tanh(a\, t_{inc})}{a\, t_{inc}} \quad \text{with} \quad a = \sqrt{\frac{-3E_m^f}{2E_{inc} \ln \xi}} \quad (13)$$

where t_{inc} is the inclusions' effective aspect ratio, equal to 1 for spherical inclusions and $t_{inc}>1$ for elliptical inclusions. C is a normalization parameter which satisfies the boundary condition $E_c=E_m$ for $V_f=0$.

The inclusion model parameters are summarized in Table 2 for zLLDPE and mLLDPE/CNT nanocomposites. Figures 2, 3 demonstrate the simulated values of the nanocomposites' elastic modulus for various values of the model parameters, in comparison with the experimental data.

Table 2
Parameters of Inclusion Model for zLLDPE/CNT and mLLDPE/CNT nanocomposites.

Material	t_{inc}	ξ	λ
zLLDPE/CNT	1	0.9	0.27
	3	0.64	0.2
	5	0.5	0.2
	5	0.43	0.3
	10	0.2	0.6
	10	0.18	0.8
mLLDPE/CNT	3	0.74	0.2
	5	0.61	0.2
	10	0.5	0.2
	10	0.5	0.28
	12	0.4	0.24

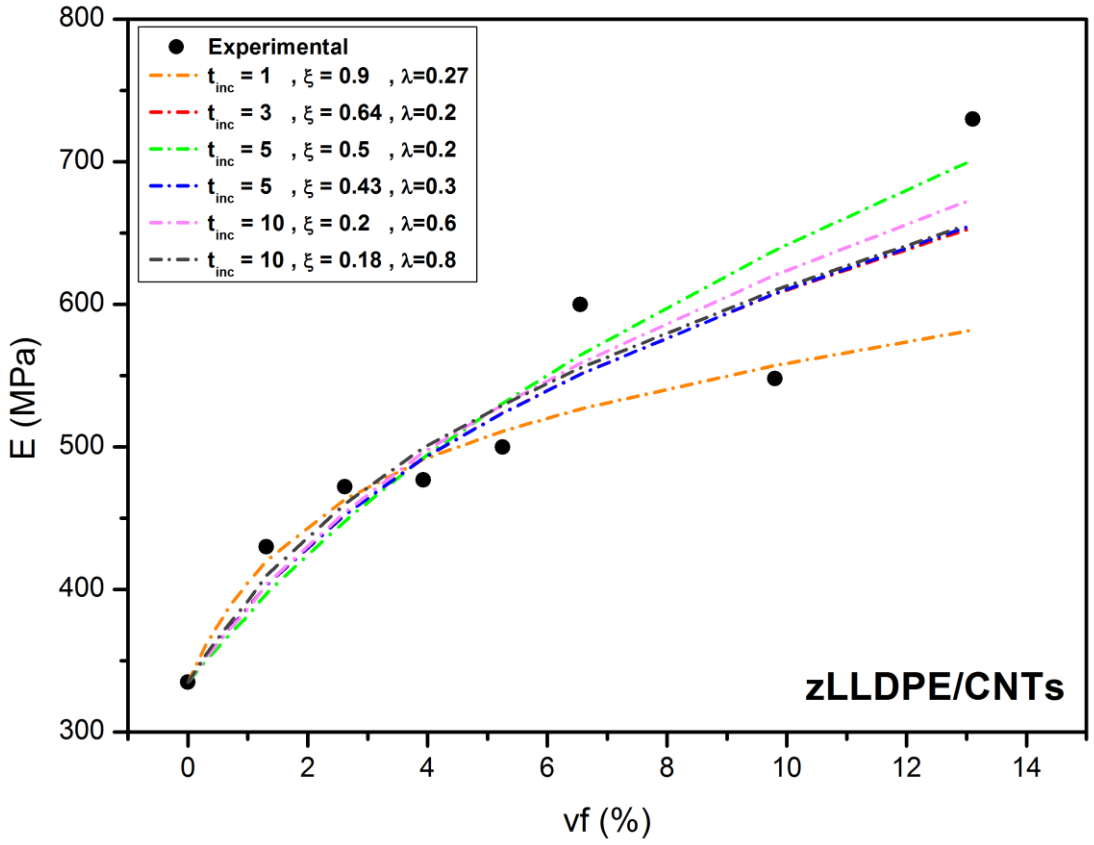

Figure 2: Variation of the Young's modulus of the zLLDPE/CNT nanocomposites with CNTs volume fraction. Lines: Inclusion model simulation at various model parameter values. Points: Experimental data taken from Ref.[6]

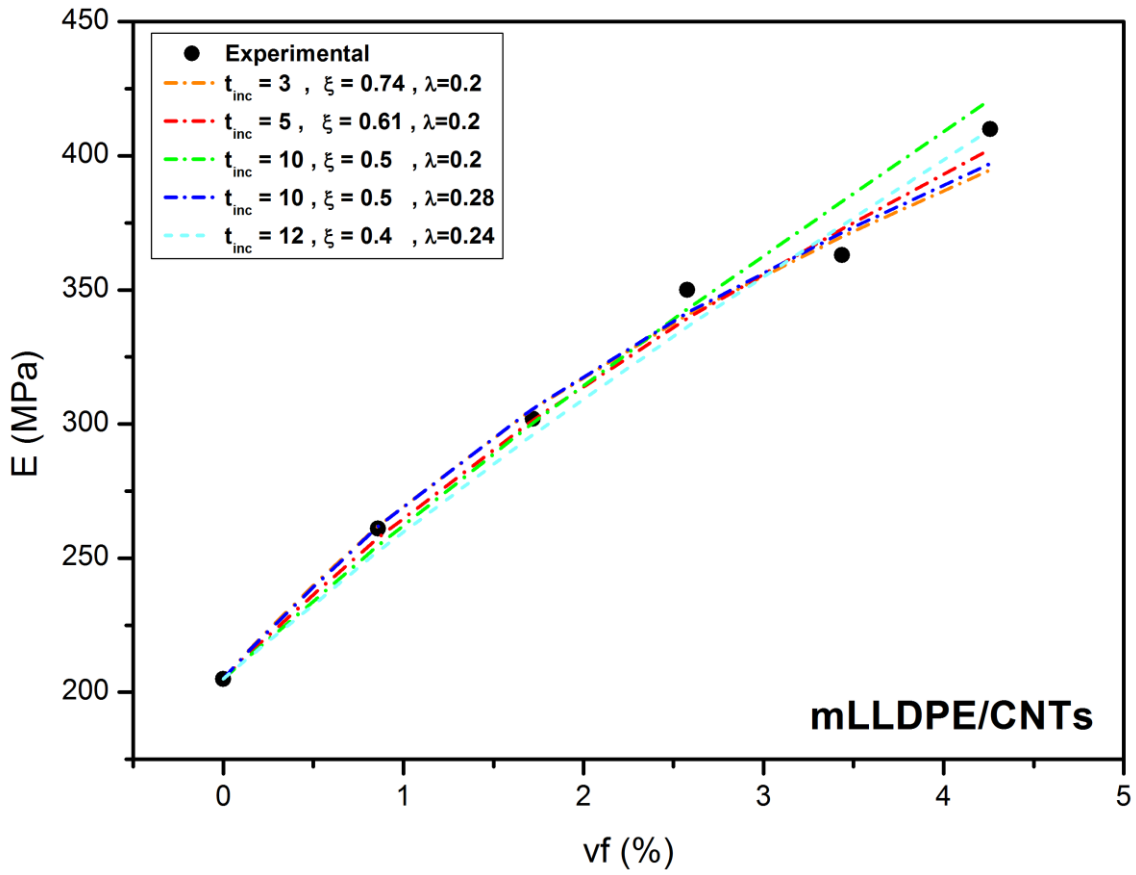

Figure 3: Variation of the Young's modulus of the mLLDPE/CNT nanocomposites with CNTs volume fraction. Lines: Inclusion model simulation at various model parameter values. Points: Experimental data taken from Ref [7].

In Figures 2 and 3, the model results with the best approximation with the experimental data are depicted, for various model parameter values. These results demonstrate the unavoidability of the CNTs agglomeration. The existence of agglomerates in the nanocomposites under investigation has been verified by scanning electron microscopy images [6,7]. The model parameter values with the best approximation to the experiments are: t_{inc} =5, ξ=0.5, λ=0.2 for zLLDPE/CNT and t_{inc} =5, ξ=0.61, λ=0.2

for mLLDPE/CNT nanocomposites. It is revealed that a high percentage of the CNTs participates to the agglomerates in both material types.

3. Finite element analysis model

In this section, the effective elastic modulus of the LLDPE/CNT nanocomposites will be analyzed in terms of two different micromechanical techniques, based on finite element analysis (FEA): an inclusion model and a three-phase model.

3.1 Inclusion model

The first procedure is based on the previously presented analytical inclusion model. The method employed is the three - step homogenization process. Following the analytical model, the pure matrix and the randomly distributed CNTs consist a new phase, called a fictitious matrix. The design and meshing of the RVE, based on this assumption are shown in Figure 4. The elastic constants of the CNTs are listed in Table 2 and the Young's modulus of the polymeric matrix is the experimental one, as obtained in our previous works [6,7] equal to 335 MPa and 205 MPa. The aspect ratio of the CNTs in zLLDPE and mLLDPE matrix was 667 and 400 respectively, equal to the nominal properties.

The second phase, the inclusion, consists of CNTs agglomerates and matrix material, and is randomly distributed into the nanocomposite. Therefore, the whole system is described by two phases, the fictitious matrix and the inclusions. The representative volume elements (RVEs) are presented in Figures 4, 5 and 6.

At the first step of the homogenization, the fictitious matrix has been modeled. The calculations were performed using the software Ansys 2019R2. The matrix was treated

as an isotropic material with a Young's modulus E_m equal to 335 MPa for the zLLDPE and 205 MPa for the mLLDPE and a Poisson's ratio equal to 0.42. The CNTs were treated as a transversely isotropic material with a longitudinal modulus equal to 910 GPa. All the engineering constants are listed in Table 3.

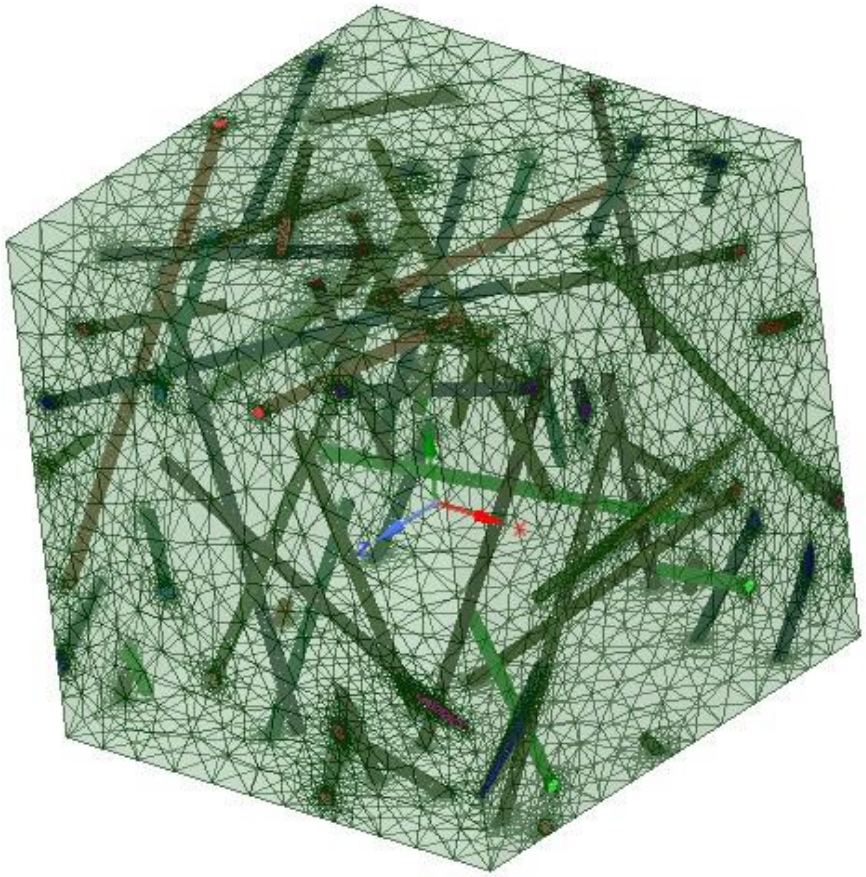

Figure 4: RVE of the fictitious matrix.

Table 3
Engineering Constants of CNTs.

E_1 (GPa)	$E_2=E_3$ (GPa)	$G_{12} = G_{13}$ (GPa)	$v_{12} = v_{13}$	v_{23}
910	304	194	0.2	0.3

It is to be noted here that the elastic constants of the CNTs employed in the FEA analysis are the same to those in the analytical model. In general, it is difficult to calculate the elastic properties of CNTs in the microstructure with perfect accuracy and molecular dynamics simulations are often used to calculate them. For this reason, the values of elastic constants chosen for CNTs are similar to those presented in [36], and employed in molecular dynamics techniques. On the basis of these values, the experimental results for the nanocomposite materials were approximated. The calibration procedure started by testing values similar to those presented in [36]. The values that gave the best approximation to the experimental results were those listed in Table 3.

At the second step of the homogenization process, the elastic stiffness of the inclusion was calculated. It was assumed that the CNTs content is the 80% of the inclusion. The same parameter values, regarding the matrix and the CNTs, as in the first step were employed. The RVE of this step is illustrated in Figure 5.

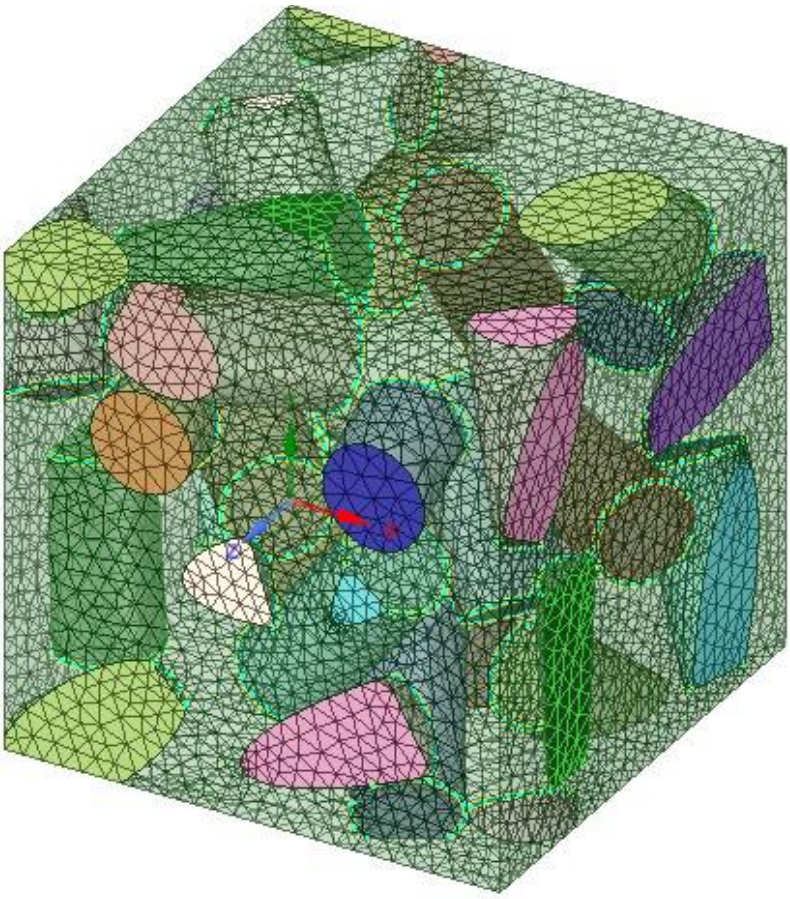

Figure 5: RVE of the inclusions

The final RVE of the nanocomposite was hereafter modeled with the known elastic constants of the fictitious matrix and the inclusions. The RVE of this step is illustrated in Figure 6. The inclusions are considered to be spherical with diameters ranging between a minimum and a maximum value equal to 175 nm and 877 nm respectively, and were treated as orthotropic materials. The parameter values are presented in Table 4, and the simulated elastic moduli of the LLDPE/CNT nanocomposites, designated as FEA-Inclusion Model, are illustrated in Figures 7,8.

Table 4
Engineering Constants of Inclusions.

Engineering Constants	zLLDPE/CNT	mLLDPE/CNT
E_1 (GPa)	851	742
E_2 (GPa)	820	724
E_3 (GPa)	762	712
G_{12} (GPa)	273	170
G_{23} (GPa)	246	158
G_{13} (GPa)	276	172
v_{12}	0.379	0.379
v_{23}	0.428	0.428
v_{13}	0.418	0.418

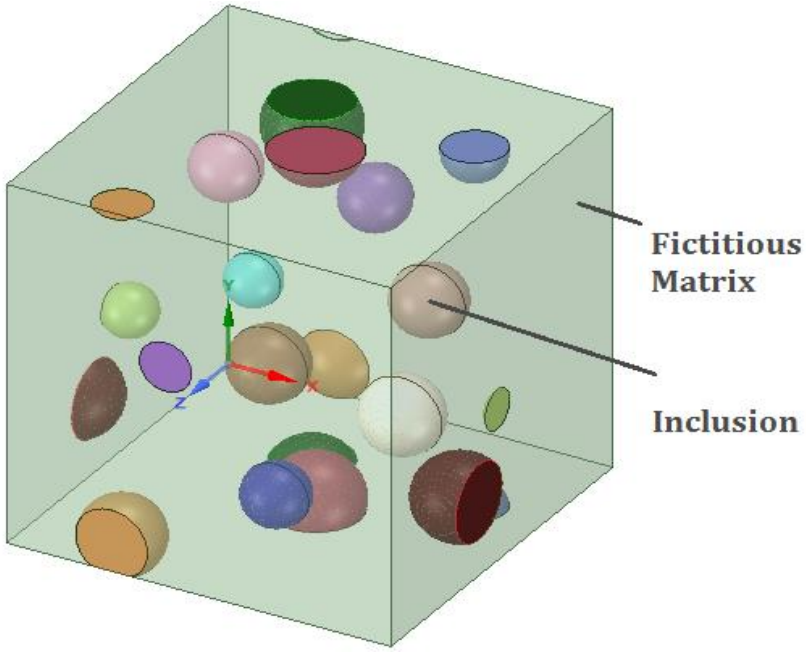

Figure 6: RVE of the nanocomposite, including the fictitious matrix and the inclusions

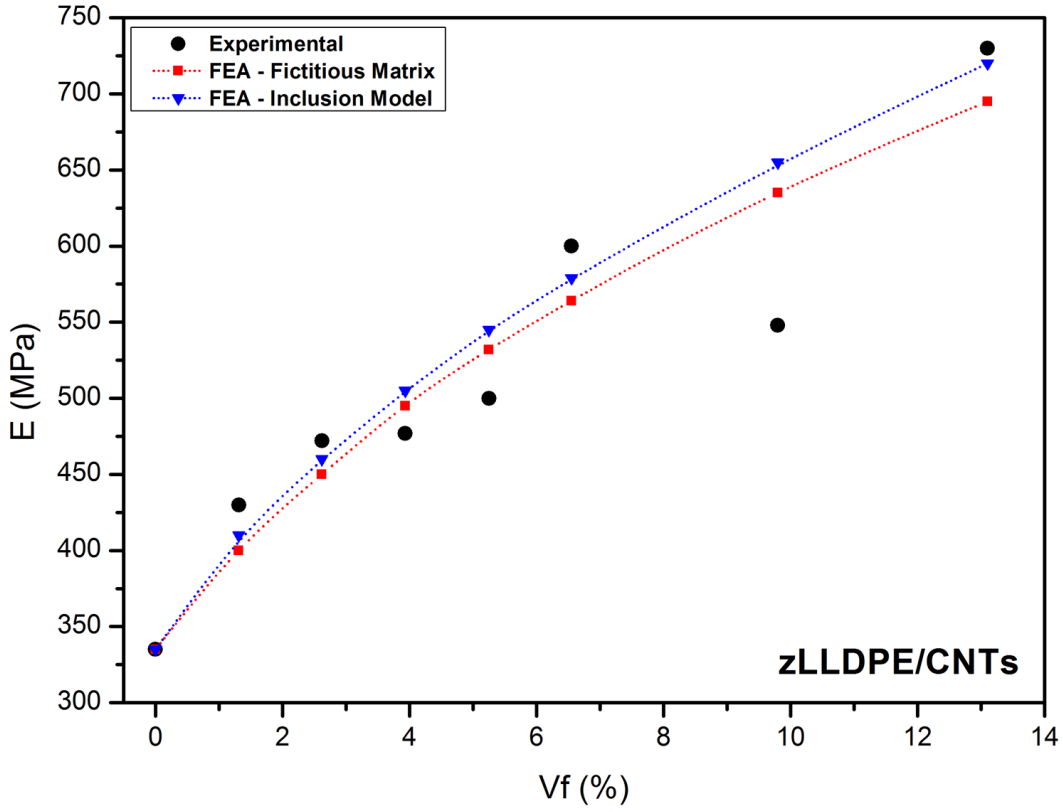

Figure 7: Variation of the Young's modulus of the zLLDPE/CNT nanocomposites with CNTs volume fraction. Lines: FEA simulation. Points: Experimental data taken from Ref [6].

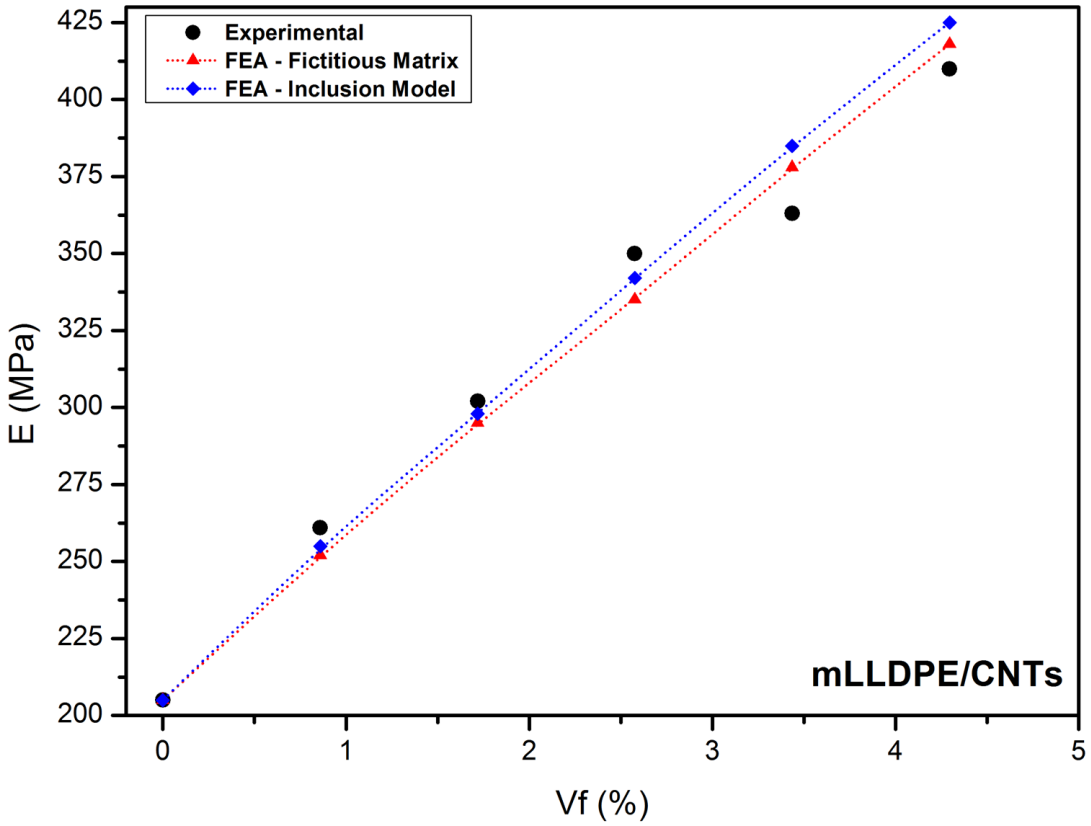

Figure 8: Variation of the Young's modulus of the mLLDPE/CNT nanocomposites with CNTs volume fraction. Lines: FEA simulation. Points: Experimental data taken from Ref [6].

To further analyze the inclusion model's capability, the LLDPE/CNT nanocomposites have been modeled as a matrix containing randomly dispersed CNTs. The whole system is now modeled in a similar way to that of the fictitious matrix, and the presence of CNTs agglomerates is not taken into account. The simulated results of this procedure, designated as FEA-Fictitious Matrix, are comparatively plotted with the FEA-Inclusion

Model, in Figures 7 and 8. From these plots, it is extracted that the presence of the CNT inclusions further reinforce the Young's modulus of the nanocomposites. In both Figures, a very good Young's modulus prediction is obtained for the nanocomposites investigated.

3.2 Three-phase model (Interphase)

The concept of the interphase, which is treated as a thin interface layer usually covering the particles in conventional composites has been extensively studied [37, 10, 17]. Having a much smaller thickness than the filler's size this layer may not greatly affect the overall properties of the composite. However, this is not the case for nanocomposites, where the nanofillers' dimensions are of the same order of those of the interphase, and there is a large-surface area between them and the matrix. Particularly in CNT/nanocomposites, the interphase is an area in which van der Waals electromagnetic forces are exerted between the polymeric matrix and CNTs. Therefore, the interphase is expected to play an important role on the mechanical enhancement of the nanocomposites [38-41]. To this trend, Li and Seidel [42] studied the load transfer ability of the interphase in CNT/epoxy nanocomposites using molecular dynamics. In addition, some new models including the interphase have been developed [43]. The interphase areas can produce connected networks, which accelerate the mechanical percolation in polymer nanocomposites at a lower volume fraction of nanoparticles. Consequently, the interphase affects the percolating role of the nanoparticles in the nanocomposites besides the reinforcing efficiency [44].

In this section, a three-phase model is considered, consisting of the polymeric matrix, CNTs randomly distributed and an intermediate region around the CNTs, the so-called

interphase region. This model is illustrated in Figure 9, where R_i, R_o are the inner and outer radii of the CNTs and R_{inter} the interphase radius. The aim of this analysis is to study the effect of the interphase and its elastic properties on the elastic stiffness of the nanocomposite. In many articles such as [45, 46] the interphase was modeled as an isotropic material with high Poisson ratio, therefore, in the present work, this region is modeled as an isotropic material with unknown properties, which are the model parameters. The polymeric matrix phase is considered an isotropic material with a Young's modulus equal to the experimental one and a Poisson's ratio equal to 0.42 [6,7]. The longitudinal modulus of the CNTs, is taken equal to 910 GPa, as in the previous sections. Following the analysis, presented in the previous paragraph, the calculation of the elastic constant $E^{m}_{RandomCNT}$ of the randomly oriented CNTs has been performed.

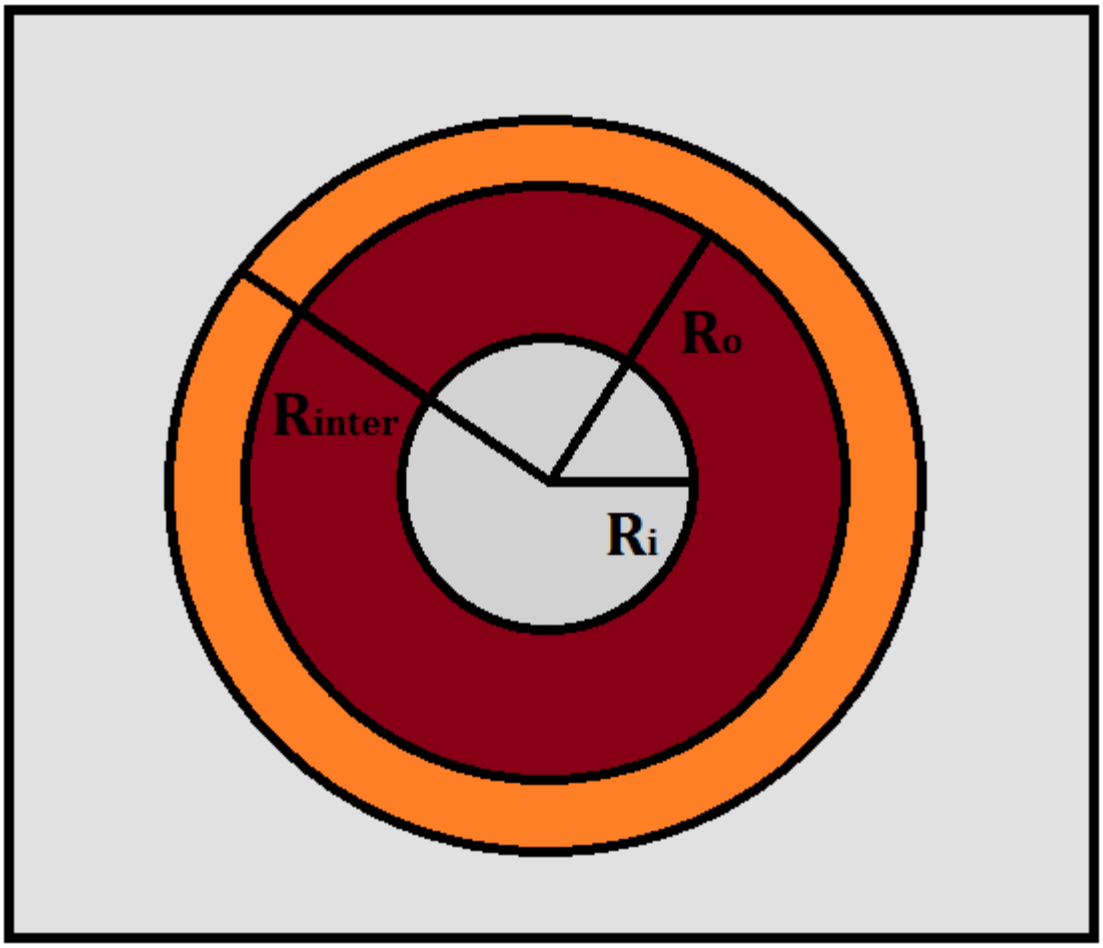

Figure 9: Three-phase (interphase) model

Following Figure 9, considering as α the side length of the RVE and L the CNT length, we have:

$$V_f = \frac{V_{CNT}}{V_{RVE}} = \frac{\pi}{\alpha^3}\left(R_o^2 - R_i^2\right)L \tag{14}$$

$$V_{inter} = \frac{V_{inter}}{V_{RVE}} = \frac{\pi}{\alpha^3}\left(R_{inter}^2 - R_o^2\right)L \tag{15}$$

$$V_m = 1 - V_{inter} - V_f \quad (16)$$

The MWCNTs employed are of R_i=2.5 nm and R_o=5 nm. From the above equations (14) to (16) we have:

$$\frac{V_{inter}}{V_f} = \frac{R_{inter}^2 - R_o^2}{R_o^2 - R_i^2} \quad (17)$$

By selecting a proper value for $R_{inter,}$ the interphase thickness is then evaluated. Considering that $\frac{V_{inter}}{V_f} < \frac{1}{2}$ it was found that R_{inter}<5.86 nm, therefore the interphase thickness t_{inter} was less than or about equal to 0.86 nm. Hereafter, selecting the interphase Young's modulus E_{inter} = 1 GPa, and applying the following well known empirical equations, the Young's modulus E_c of the nanocomposite can be extracted as:

$$E_c = E^m_{RandomCNT}(1 - V_{inter}) + E_{inter} V_{inter} \quad (18)$$

where $$E^m_{RandomCNT} = E_m V_m + E_f^{eff} V_f \quad (19)$$

with E_f^{eff} = 910 GPa, and $V_f + V_m + V_{inter} = 1$

The interphase thickness will assume the values 0.2, 0.4, 0.6 and 0.8 nm.

The results of this analysis are shown in Figures 10 to 13 for both LLDPE/CNT nanocomposites and various model parameter values, in comparison with the experimental results.

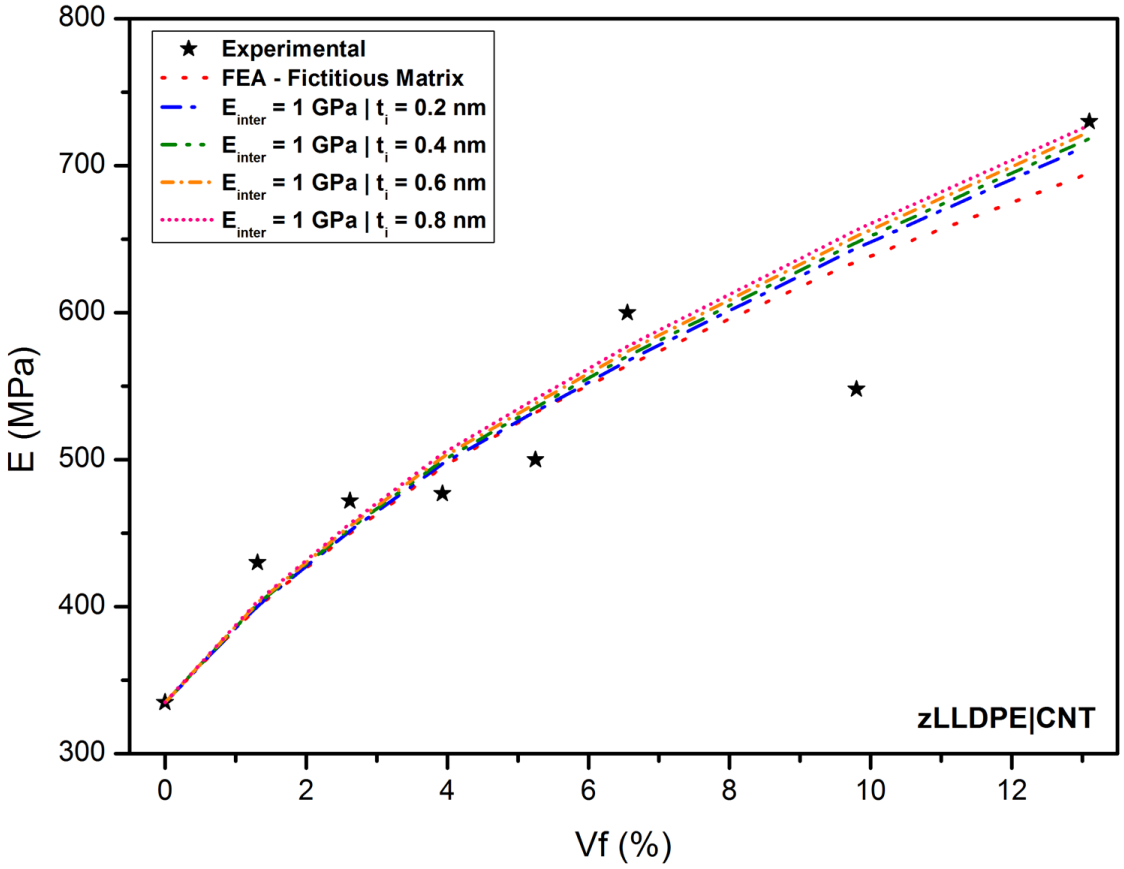

Figure 10: Variation of the Young's modulus of the zLLDPE/CNT nanocomposites with CNTs volume fraction. Dashed lines: Three-phase model simulation at various interphase thickness values, against FEA-Fictitious Matrix model. Points: Experimental data taken from Ref [6].

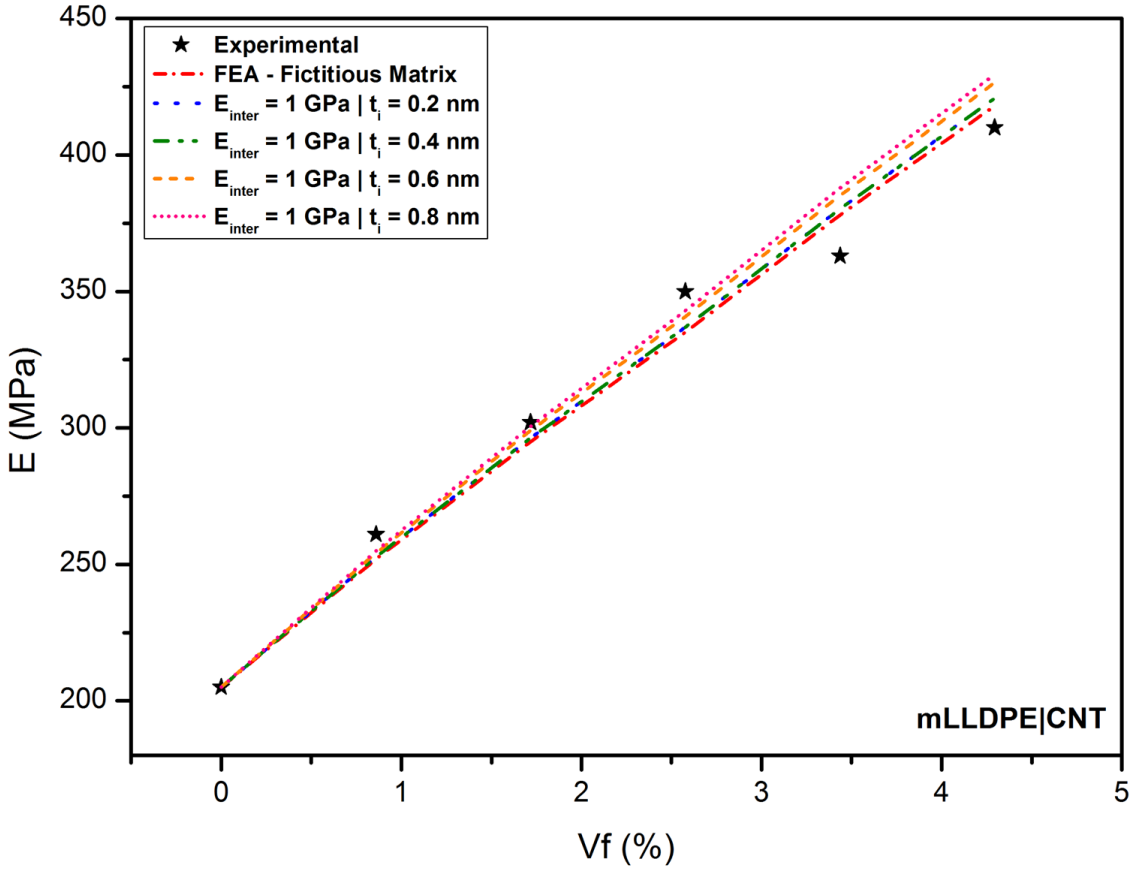

Figure 11: Variation of the Young's modulus of the mLLDPE/CNT nanocomposites with CNTs volume fraction. Dashed lines: Three-phase model simulation at various interphase thickness values, against FEA-Fictitious Matrix model. Points: Experimental data taken from Ref [7].

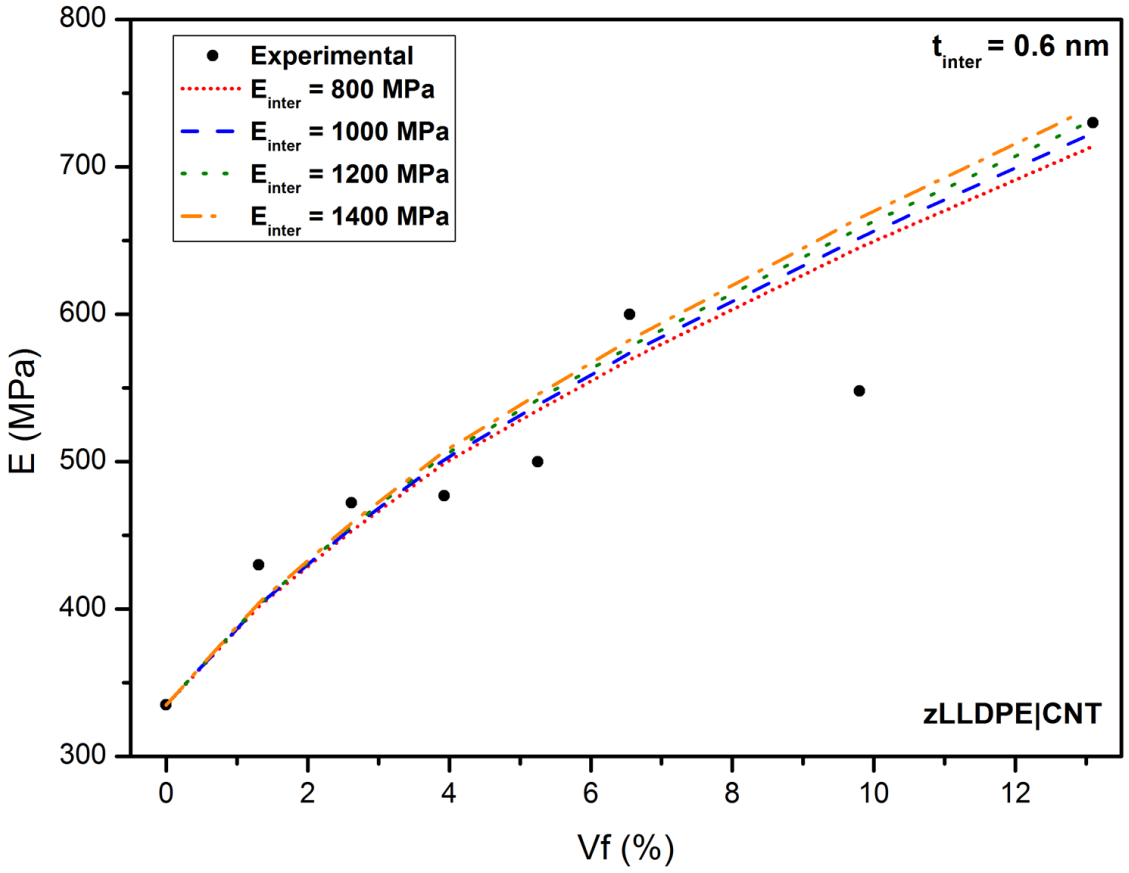

Figure 12: Variation of the Young's modulus of the zLLDPE/CNT nanocomposites with CNTs volume fraction. Dashed lines: Three-phase model simulation at various values of the interphase modulus. Points: Experimental data taken from Ref [6].

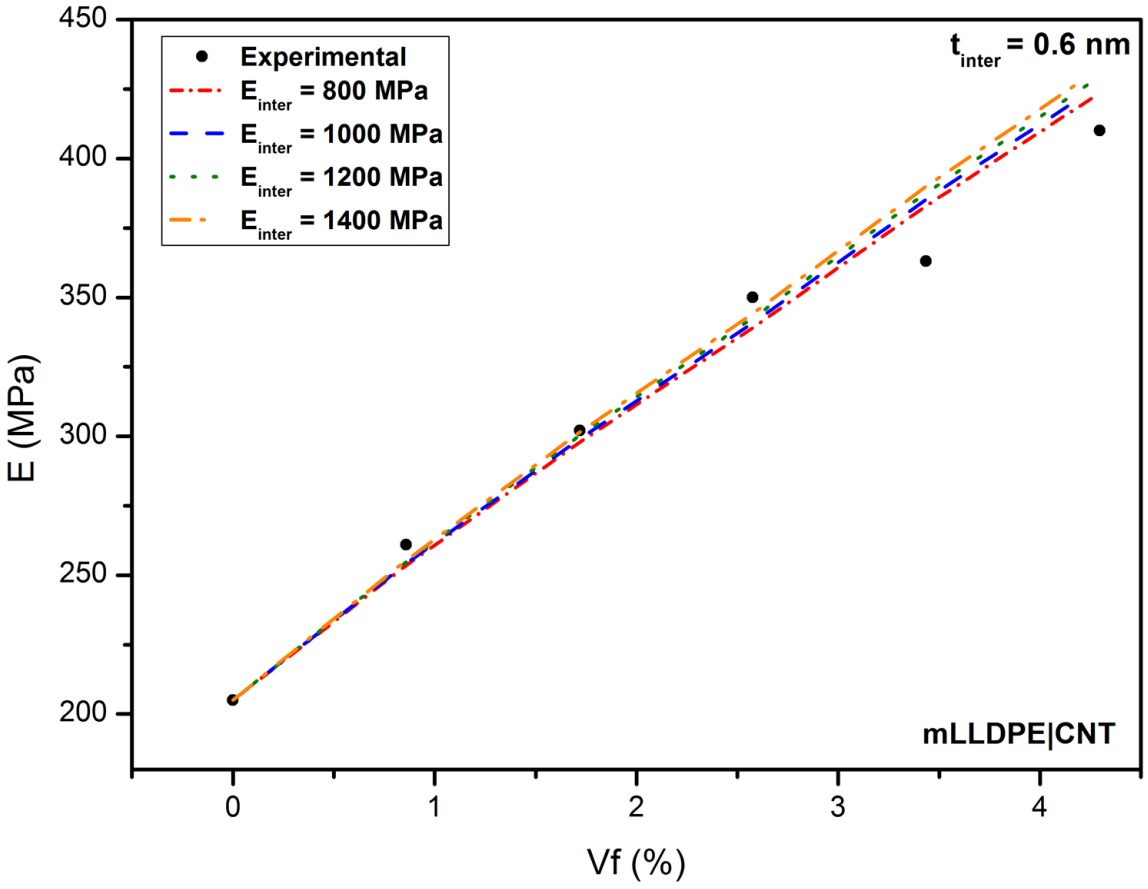

Figure 13: Variation of the Young's modulus of the mLLDPE/CNT nanocomposites with CNTs volume fraction. Dashed lines: Three-phase model simulation at various values of the interphase modulus. Points: Experimental data taken from Ref [7].

In Figures 10 to 13, a good approximation between model simulation and experimental data is obtained. Furthermore, with increasing E_{inter} at the same interphase thickness the Young's modulus increases. In addition, with increasing interphase thickness, at the same E_{inter} value, the Young's modulus increases. From the above results, it can be extracted that the best simulation is achieved with E_{inter}=1 GPa and t_{inter}=0.5 nm.

In Figures 10 and 11 the FEA-Fictitious Matrix model simulations, as presented in section 3.1, are comparatively depicted. From these comparative plots, it is obtained that this assumption leads to lower stiffness values, revealing the important role of the interphase in the mechanical enhancement. In particular, this effect is more clearly shown in Figure 11 for the mLLDPE/CNT nanocomposites, where the interphase model exhibits a better approximation to the experimental results than the FEA-Fictitious Matrix model.

4. Conclusions

In the present work, a new model is proposed for the prediction of the effective modulus of two types of polymer/CNT nanocomposites. On the basis of the inherent tendency of CNTs to agglomerate, the material is considered to be a two-phase system consisting of a fictitious matrix (itself consisting of the matrix and dispersed CNTs) and the inclusions, which are based on the CNTs agglomerates. To analyze the effective modulus of the fictitious matrix, Odegard's method of the effective fiber is employed, therefore the proposed analysis incorporates both the inherent tendency of the CNTs to agglomerate and the role of the interphase region around CNTs, given the large surface area between the matrix and the nanofillers. The inclusions' modulus is evaluated by an empirical model, including two aggregation parameters. Finally the effective modulus

of the nanocomposite is obtained by the Cox-Krenchel equation. The CNTs were treated as transversely isotropic, and the model simulations were in good agreement with the experimental data. According to the results, the CNTs agglomeration is unavoidable and decisive to the mechanical enhancement. The inclusion model was further analyzed through finite element analysis, and a comparison has been performed with the results obtained by considering random distribution of CNTs. It was found that the inclusion model leads to higher stiffness values than those with the CNTs randomly distributed into the matrix, and closer to the experimental results.

Given that the region between the CNTs and the matrix, the so-called interphase, is characterized by its own properties, and was proved to play a decisive role on the nanocomposites' reinforcement, an additional analysis has been performed by a three-phase model using finite element analysis. A parametric study has been made to examine the effect of the interphase thickness and stiffness on the mechanical performance of the nanocomposites. A good approximation with the experimental data has been obtained. The research findings of the present work reveal that the proposed analytical inclusion model is capable of predicting the elastic modulus of the polymer nanocomposites. In addition, FEA procedure based on the proposed analytical model leads to nearly identical results. The concept of the inclusion appears to be crucial for the description of the nanocomposites mechanical enhancement.

References

[1] E.T. Thostenson, Z. Ren, T.W.Chou, Advances in the science and technology of carbon nanotubes and their composites:a review, Compos. Sci. Techn. 61(13) (2001) 1899-1912.

[2] VahidTahouneh, Mahmoud Mosavi Mashhadi, Mohammad Hasan Naei, Finite element and micromechanical modeling for investigating effective material properties of polymer–matrix nanocomposites with microfiber, reinforced by CNT arrays, Int. J. Adv. Struct. Eng. 8 (2016) 297-306. DOI 10.1007/s40091-016-0132-y

[3] F.T. Fisher, R.D. Bradshaw1, L.C. Brinson, Fiber waviness in nanotube-reinforced polymer composites—I: Modulus predictions using effective nanotube properties, Composites Science and Technology 63 (2003) 1689–1703. doi:10.1016/S0266-3538(03)00069-1

[4] R.D. Bradshaw1, F.T. Fisher, L.C. Brinson, Fiber waviness in nanotube-reinforced polymer composites—II:modeling via numerical approximation of the dilute strain concentration tensor, Composites Science and Technology 63 (2003) 1705–1722, doi:10.1016/S0266-3538(03)00070-8

[5] M. Bhattacharya, Polymer Nanocomposites—A Comparison between Carbon Nanotubes, Graphene, and Clay as Nanofillers, Materials, 9, 262 (2016). Doi: 10.3390/ma9040262.

[6] G.Georgousis, I.Charitos,E.Kontou, S.Koutsoumpis, Z.Terzopoulou, D.Bikiaris, Thermomechanical-electrical properties and micromechanics modeling of linear low density polyethylene reinforced with multi-walled carbon nanotubes, Polymer Composites 2018, DOI 10.1002/pc.24584.

[7] I.Charitos, G.Georgousis, E.Kontou, Preparation and Thermomechanical Characterization of Metallocene Linear Low-Density Polyethylene/Carbon Nanotube Nanocomposites, Polymer Composites 2019, DOI 10.1002/pc.24961.

[8] Y. Wu, Z. Gu, M. Chen, et al., Effect of functionalization of multi-walled carbon nanotube on mechanical and viscoelastic properties of polysulfide-modified epoxy nanocomposites, High Perform. Polym. 29 (2017) 151–160.

[9] Y.Liu, X. Chen X, Evaluations of the effective material properties of carbon nanotube-based composites using a nanoscale representative volume element, Mech. Mater. 35(1) (2003) 69–81.

[10] G.M. Odegard, T.S.Gates, K.E.Wise, C. Park, E.J.Siochi, Constitutive modeling of nanotube-reinforced polymer composites, Compos. Sci. Technol. 63 (2003)1671–1681.

[11] Y. Benveniste**,** A new approach to the application of Mori-Tanaka's theory in composite materials, Mech. Mater., 6, (1987) 147-157.

[12] G.D. Seidal, D.C. Lagoudas, Micromechanical analysis of the effective elastic properties of carbon nanotube reinforced composites, Mech. Mater. 38 (2006) 884–907.

[13] V.Anumandla, R.F. Gibson, A comprehensive closed form micromechanics model for estimating the elastic modulus of nanotube-reinforced composites, Compos. A 37 (2006) 2178–2185.

[14] S. Kanagaraj, F.R. Varanda, T.V. Zhil'tsova , M.S.A. Oliveira, and J.A.O. Simões, Mechanical properties of high density polyethylene/carbon nanotube composites, Compos. Sci. Techn., 67**,** (2007) 3071-3077.

[15] Meisam Omidi , Hossein Rokni D.T., Abbas S. Milani, Rudolf J. Seethaler, R. Arasteh, Prediction of the mechanical characteristics of multi-walled carbon nanotube/epoxy composites using a new form of the rule of mixtures, Carbon 48 (2010) 3218-3228. doi:10.1016/j.carbon.2010.05.007

[16] B. Arash, Q. Wang & V. K. Varadan, Mechanical properties of carbon nanotube/polymer composites, Scientific reports (2014). DOI: 10.1038/srep06479.

[17] Shenggui Chen, Mohsen Sarafbidabad, Yasser Zare and Kyong Yop Rhee, Estimation of the tensile modulus of polymer carbon nanotube nanocomposites containing filler networks and interphase regions by development of the Kolarik model, RSC Adv. 8 (2018) 2382523834. DOI: 10.1039/c8ra01910j.

[18] Yasser Zare, Kyong Yop Rhee, Tensile modulus prediction of carbon nanotubes-reinforced nanocomposites by a combined model for dispersion and networking of nanoparticles, J. of Mater. Res. And Technol. (2019). https://doi.org/10.1016/j.jmrt.2019.10.025

[19] Unnati A. Joshi, Preeti Joshi, S. P. Harsha, Satish C. Sharma, Evaluation of the Mechanical Properties of Carbon Nanotube Based Composites by Finite Element Analysis, International Journal of Engineering Science and Technology, 2(5) (2010) 1098-1107.

[20] A. K. Manta and K. I. Tserpes, Parametric numerical simulation of impact response of carbon nanotube/polymer nanocomposites Parametric numerical simulation of impact response of carbon nanotube/polymer nanocomposites, Plastics, Rubber and Composites 45(4) (2016) 157-165. DOI: 10.1080/14658011.2016.1152652.

[21] Anuj Kumar Singh,S. P. Harsha, A Parashar, Finite Element Analysis of CNT reinforced epoxy composite due to Thermo-mechanical loading, Procedia Technology 23 (2016) 138 – 143.

[22] J-h. Tai, G-q. Liu, H. Caiyi, and S. Lin-jian, Mater. Res. 15 (2012) 1050- DOI10.1590/S1516–14392012005000122.

[23] J. Aalaie, A. Rahmatpour, and S. Maghami, Preparation and characterization of linear low density polyethylene/carbon nanotube nanocomposites, J. Macromol. Sci. Phys. B, 46 (2007) 877-889. DOI.org/10.1080/00222340701389100.

[24] M.T. Müller, B. Krause, P. Pötschke, A successful approach to disperse MWCNTs in polyethylene by melt mixing usingpolyethylene glycol as additive, Polymer 53 (2012) 3079-3083. doi:10.1016/j.polymer.2012.05.041.

[25] A.A. Vasileiou, A. Docoslis, M. Kontopoulou, P. Xiang, and Z. Ye, The role of non-covalent interactions and matrix viscosity on the dispersion and properties of LLDPE/MWCNT nanocomposites,Polymer, 54, (2013) 5230-5240.

[26] A.A. Vasileiou, A. Docoslis, and M. Kontopoulou, A comparison of LLDPE-based nanocomposites containing multi-walled carbon nanotubes and graphene Proceedings of PPS-30, AIP Conference Proceedings 1664, 070017–1–070017-5 (2015). doi: 10.1063/1.4918452

[27] T. Mori , and K.Tanaka, Average stress in matrix and average elastic energy of materials with misfitting inclusions, Acta Metallurgica, 21 (1973) 571-574.

[28] E. Kontou and M.Niaounakis, Thermo-mechanical properties of LLDPE/SiO2nanocomposites, Polymer, 47 (2006) 1267-1280.

[29] G. Georgousis , K. Roumpos , E. Kontou, A. Kyritsis, P. Pissis, S. Koutsoumpis,

M. Mičušík, M. Omastová, Strain and damage monitoring in SBR nanocomposites under cyclic Loading, Composites Part B, 131 (2017) 50-61, http://dx.doi.org/10.1016/j.compositesb.2017.08.006

[30] Jing Pan , Lichun Bian, Influence of agglomeration parameters on carbon nanotube Composites, Acta Mech. 228 (2017)2207–2217 .DOI 10.1007/s00707-017-1820-9

[31] J.D. Eshelby, Proceedings of the Royal Society of London, Series A, A241, 376 (1957).

[32] T. Mura, Micromechanics of defects in solids. The Hague:Martinus Nijhoff (1982).

[33] S.Tsai, and N. Pagano, (1968). In: Composite Materials Workshop, Lancaster, PA, 233.

[34] J.C. Halpin, and N.J.Pagano,The laminate approximation for randomly oriented fibre composites, J. Compos. Mater. 3 (1969) 720-724.

[35] H.L.Cox, The elasticity and strength of paper and other fibrous materials. British Journal of AppliedPhysics,3(3), (1952)72–79. doi:10.1088/0508-3443/3/3/302.

[36] M. M. Zaeria, S. Ziaei-Rada , A. R. Shahidia , On the Elastic Constants of Single Walled Carbon Nanotubes, Elsevier ,DOI: 10.1016/j.mspro.2015.11.021.

[37] G. C. Papanicolaou, A. G. Xepapadaki, E. D. Drakopoulos, K. P. Papaefthymiou, D. V. Portan, Interphasial Viscoelastic Behavior of CNT Reinforced Nanocomposites Studied by Means of the Concept of the Hybrid Viscoelastic Interphase, J Applied Polymer Science, 124 (2012)1578-1588. DOI 10.1002/app.35202

[38] C. Wan and B. Chen, Reinforcement and interphase of polymer/graphene oxide nanocomposites, J. Mater. Chem., 22 (2012) 3637–3646.

[39] R. Razavi, Y. Zare and K. Y. Rhee, A model for tensile strength of polymer/carbon nanotubes nanocomposites assuming the percolation of interphase regions, Colloids Surf., A. 538 (2018) 148–154.

[40] Y. Zare and K. Y. Rhee, Development of Hashin–Shtrikman model to determine the roles and properties of interphases in clay/CaCO3/PP ternary nanocomposite, Appl. Clay Sci., 137 (2017) 176–182.

[41] T. Tsafack, J.M. Alred, K.E. Wise, B. Jensen, E. Siochi, B.I. Yakobson, Exploring The interface between single-walled carbon nanotubes and epoxy resin, Carbon 105 (2016) 600–606.

[42] Y.Li, G.D. Seidel, Multiscale modeling of the interface effects in CNT-epoxy Nanocomposites, Computational Materials Science 153 (2018) 363–381, https://doi.org/10.1016/j.commatsci.2018.07.015.

[43] A. Montazeri and R. Naghdabadi, Investigation of the interphase effects on the mechanical behavior of carbon nanotube polymer composites by multiscale modeling, J. Appl. Polym. Sci., 117 (2010) 361–367.

[44] J.-M. Zhu, Y. Zare and K. Y. Rhee, Analysis of the roles of interphase, waviness and agglomeration of CNT in the electrical conductivity and tensile modulus of polymer/ CNT nanocomposites by theoretical approaches, Colloids Surf., A., 539 (2018) 29–36.

[45] Yağmur Ateşcan, Hülya Cebeci,Cameron M. Hadden , Gregory M. Odegard, Molecular Dynamics and Finite Element Investigation of Polymer Interphase

Effects on Effective Stiffness of Wavy Aligned Carbon Nanotube Composites, AIAA 2015-0701. http://doi.org/102514/6.2015-0701.

[46] Mahmood M. Shokrieh, Roham Rafiee, On the tensile behavior of an embedded carbon nanotube in polymer matrix with non-bonded interphase region ,Elsevier, DOI:10.1016/j.compstruct.2009.09.033.